Polyurethane-Inspired CO_2 Chemisorbent: Ab Initio Reaction Profiles

Vitaly V. Chaban

Independent Scientist, Russian Federation. Email address: vvchaban@gmail.com

Abstract:

Polyurethane (PU) and its numerous fine-tuned derivatives are widely employed as CO_2 scavengers thanks to (1) physisorption and (2) functionalization of the PU backbone with other CO_2 sorbents. In the present work, it has been unraveled why PU cannot exhibit CO_2 chemisorption, despite possessing the nitrogen docking sites and exhibiting strong electrostatic sorbent-sorbate interactions. Furthermore, a few types of spatial separation of the active sorption sites have been proposed to unleash the chemisorption functionality of PU. By comparing various structural modifications of PU by using the in-silico methodology, we have identified that CO_2 chemisorption by PU takes place in the case of implementing methyl and ethyl fragments between the oxygen and nitrogen atoms of PU. Herewith, the introduction of the ethyl moiety even makes CO_2 chemisorption energetically favorable relative to physisorption. The reported specific progress on materials design represents an obvious practical value for chemical engineers developing inexpensive CO_2 scavengers.

Keywords:

Polyurethane; carbon dioxide; CO_2 capture; chemisorption.

TOC Graphic

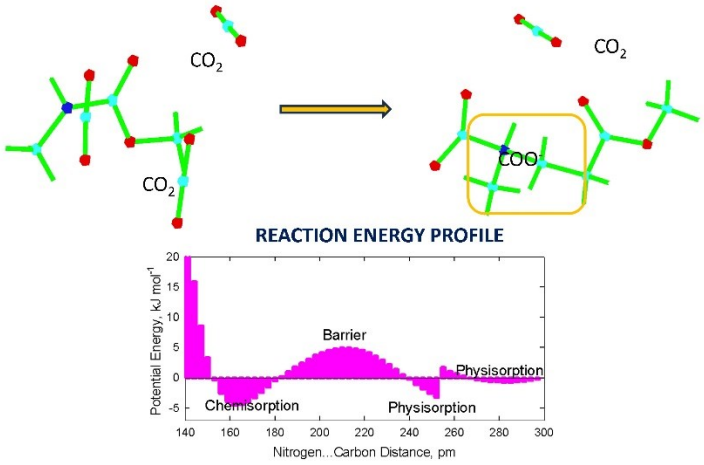

Insertion of the ethylene chain between the -N(H)- and -C(O)O- groups unleashes CO_2 chemisorption.

Research Highlights

The polyurethane chemisorption functionality has been unleashed.

The spatial separation of O and N atoms in PU enables CO_2 chemisorption.

The ethylene separator has been shown to offer the best chemisorption performance.

Introduction

The excess concentration of CO_2 in the atmosphere of the Earth represents a widely publicly discussed environmental peril nowadays due to its connection to global warming and climate alteration.[1-3] The consensus is that the emissions of human-associated greenhouse gases (methane and carbon dioxide) must be diminished to support a safer future. Numerous research teams around the globe develop novel materials exhibiting the functionality of CO_2 scavengers. The goals are to get an energetically efficient, cheap, and renewable CO_2 adsorbent and/or absorbent.[4]

Chemistry-wise, the problem of CO_2 capturing is challenging because of the thermodynamic and kinetic stabilities of this gas.[5-6] The enthalpic gain obtained due to covalent bonding with CO_2 must be large enough to compensate for the entropic penalty due to decreased conformational flexibility of the captured gas molecule. There are a relatively small number of covalent bonds, which CO_2 forms with its potential sorbents. Therefore, modern optimization of CO_2 scavengers relies on minor optimization of the scavenging material to preserve kinetic stability and minimize sorption and desorption costs at given thermodynamic conditions. Many natural and cheaply produced materials compete for being selected as CO_2 scavengers in industrial settings.[2]

Polyurethanes (PUs) designate a class of versatile polymers that are extensively used thanks to their noteworthy mechanical properties, durability, and resistance to environmental factors. PUs are synthesized by the reaction of polyols and isocyanates.[7] PUs are known to maintain different forms, including rigid foams, flexible foams, elastomers, adhesives, coatings, and sealants. The practical applications of PUs range from furniture and automotive parts to insulation materials and kitchenware as sponges.

A peculiar urethane functional group, -NHC(O)O-, combines three highly active chemical elements of the second period and the hydrogen atom.[8-11] The urethane group is formed by the reaction between an isocyanate, -NCO, and a hydroxyl group, -OH. The presence of the isocyanate moiety in the backbone is the defining feature of polyurethanes. The urethane group readily

participates in hydrogen bonding, which significantly enhances the mechanical strength, elasticity, and thermal stability of the material. Urethane groups are responsible for the excellent adhesion properties of coatings and adhesives produced out of PU. The urethane group interacts with water, acids, and bases and can undergo hydrolysis under certain conditions.[12-13] Therefore, the chemical and physical properties of PUs degrade over time due to prolonged exposure to CO_2, moisture, and aggressive agents, which are frequently present in CO_2-containing streams. This could limit the long-term effectiveness of PUs in CO_2 scavenging applications.

The interaction with CO_2 takes place through electrostatic attraction forces.[14] This leads to physical adsorption, whose intensity depends on the surrounding chemical structures possessing nucleophilic and electrophilic reaction sites. PUs can be functionalized to go beyond the chemical functionality of the backbone. For instance, amine moieties or anionic fragments derived from ionic liquids can be grafted to enhance the affinity of the material to CO_2. Carbamate and bicarbonate species emerge upon CO_2 chemisorption while utilizing such fine-tuned derivatives.[14]

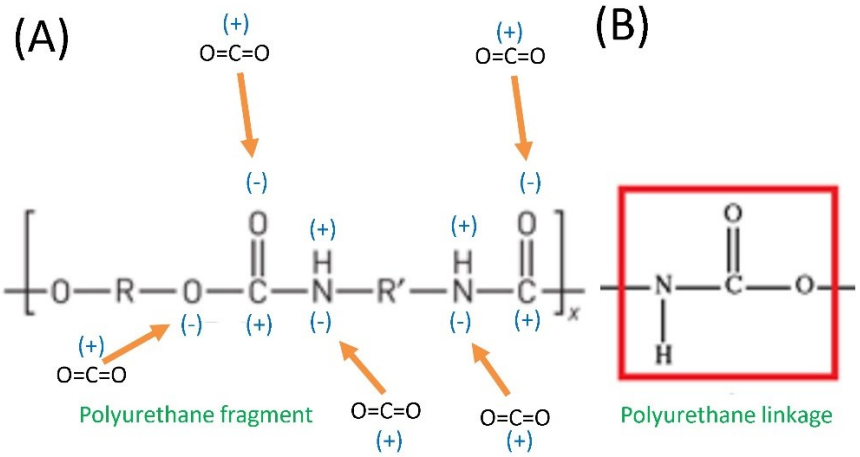

Figure 1. (A) Expected physisorption interactions of PU fragment with the CO_2 molecules. (B) Polyurethane linkage, -HNC(O)O-.

Certain types of open-cell PU foams with high surface areas and hierarchical porosity offer a great promise to physically adsorb CO_2 through the combining effect of Coulombic forces and van der Waals forces.[15-17] The large surface area provided by the PU foam structure fosters contact

between the CO_2 molecules and irregular polymer. Non-covalent interactions with a few PU chains simultaneously boost the efficiency of the capture. The CO_2 capture via physisorption is less selective but can still be effective for capturing CO_2 under specific conditions. Physisorption is widely perceived as a method with lower desorption energy costs as compared to CO_2 chemisorption. Tailorability is the cornerstone advantage of PUs as a functional material. Compared to sorptive materials for competitive CO_2 capture technologies, PUs are produced at a relatively low cost. Cheapness makes PUs one of the most attractive options for large-scale deployment.

In the present work, we use a computational methodology to solve two paramount issues related to the CO_2 chemisorption of PUs. First, we prove the principal impossibility of the non-functionalized PU to chemically absorb CO_2 due to the repulsive interaction between the oxygen atom of CO_2 and the oxygen atom of the carboxyl moiety at some point along the path of CO_2 towards the imine moiety of PU. We describe the unfavorable intermolecular O…O interaction and precisely characterize it in energetical and geometrical units. Second, we investigate minor structural modifications to potentially unleash the CO_2 chemisorption potential of PUs. Such straightforward modifications were determined at the level of in-silico atomistically precise design of materials and comprehensively characterized in terms of reaction thermochemistry, polarities of the reacting sites, and structural descriptors.

Methodology and Methods

The reaction energy profiles, containing the transition state, were obtained by forcibly moving the assigned reaction coordinate from the CO_2 gaseous state through the state of CO_2 physisorption toward the state of CO_2 chemisorption. The most intuitive reaction coordinate corresponding to the CO_2 chemisorption, carbon(CO_2)…nitrogen(PU) distance, was selected. The vibrational frequency calculations and the intrinsic reaction coordinate simulations were afterward

employed to confirm that the transition state units the physisorption state to the chemisorption state. A valid transition state must represent the first-order saddle point and contain a single vibrational frequency in its vibrational profile.

The reaction coordinate was propagated forcibly by decreasing the value of the linear reaction coordinate stepwise, by 3 pm, in all simulated chemical compositions. At each point of the energy profile, the value of the reaction coordinate was kept rigidly fixed. In turn, all other degrees of freedom of the system were allowed to adapt to the running reaction coordinate. This procedure is well-known as a relaxed energy scan in various contexts.

All recorded reaction profiles contain at least, one stationary point. This is the state of CO_2 physisorption. If an additional minimum state exists at the reaction coordinate value smaller than 200 pm, it is assigned as a CO_2 chemisorption state. The mentioned distance criterion is computed as 1.4 multiplied by the expected length of the carbon(CO_2)-nitrogen(PU) covalent bond. Furthermore, this criterion suggests an expected location of the reaction transition state This is a rule of thumb that the bond formation/bond breaking transition state is located around 130-140% of the equilibrium bond length.

The stationary points are characterized by covalent bond lengths, non-covalent interatomic distances, covalent angles, and partial atomic electrostatic charges as measures of reaction sites' nucleophilicity and electrophilicity. The partial atomic electrostatic charges are derived by fitting the electrostatic potential for electrons and atomic nuclei using the Merz-Kollman algorithm.[18] The thermodynamic potentials – Gibbs free energy, enthalpy, and configurational entropy[19] are computed at various temperatures and pressures – for CO_2 physisorption and CO_2 chemisorption using the sequence of Hess' law. The electronic energy-based heights of the obtained activation barriers are corrected correspondingly. Herewith, the physisorption thermodynamics is computed versus an ideal gas state of CO_2, i.e. the CO_2-CO_2 attraction is ignored. The corrections for zero-point energy are computed in every stationary point through the harmonic frequency analysis. The

anharmonic frequency analysis is also performed in several systems to assess the cost of the approximation for the accuracy of the results. The energetic effects of the electronic excitations are not included in these calculations.[19]

Unrestricted hybrid density functional theory (HDFT), as implemented in the range-separated exchange-correlation meta-GGA functional M11,[20] is used. The molecular wave functions rely on the primitive orbitals belonging to the atom-centered triple-zeta split-valence polarized Def2-TZVP basis set.[21] The dispersive attraction is included inherently.[20] The convergence criterion within the self-consistent field procedure was set to 10^{-7} hartree. The rational function optimization algorithm is used to optimize partially restrained geometries along the proposed minimum reaction path. The following geometry convergence criteria were chosen: 120 kJ/nm for the largest force and 40 kJ/nm for root-mean-squared force.

The HDFT calculations were conducted in GAMESS.2020.[22] The in-house scripts were utilized to carry out all other analysis routines. The Avogadro drag-and-drop software was used to draw preliminary molecular geometries of the simulated chemical structures.[23]

Results and Discussion

In this section, we first show that pristine PU does not chemically absorb CO_2. The scavenger's performance of PU is exclusively due to numerous pairwise electrostatic attractions, primarily involving electrophilic carbon atoms in CO_2 and carboxylate moieties. Next, we modify the structure of PU aiming to avoid unfavorable intermolecular interactions that prevent chemical absorption. The modifications appear to be successful and unleash the desired new functionality, which is characterized in terms of kinetic and thermochemical descriptors.

Chemisorption of CO_2 in Polyurethane

Figure 2 depicts the absence of CO_2 chemisorption in pristine PU and visualizes key non-covalent interactions, which influence this sort of system behavior. No activation energy barrier that could separate the state of CO_2 chemisorption from the state of CO_2 physisorption was identified. Therefore, no chemisorption state exists as well. Even if such a state is attained during thermal motion at the temperature of CO_2 capture, it is spontaneously destroyed during microscopic time frames at any finite translational temperature.

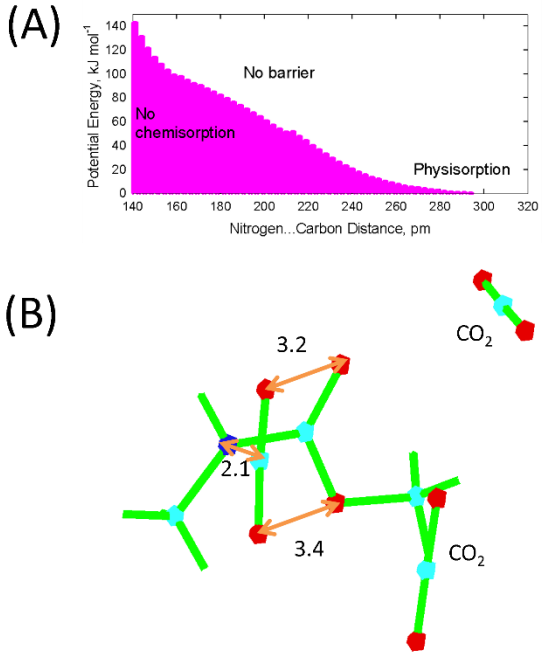

Figure 2. (A) Computed CO_2 chemisorption energy profile for PU. (B) Electrostatic oxygen-oxygen repulsions, preventing CO_2 chemisorption by PU. The in-plot distances are given in Ångstroms.

The partially optimized geometry of the simulated system, containing one urethane unit and three CO_2 molecules, is depicted in Figure 2b to rationalize the reaction energy profile in Figure 1a. At the reaction coordinate of 214 pm, the two oxygen atoms of the approaching CO_2 meet the two oxygen atoms of the urethane linkage, which is an inherent part of the sorbent. The corresponding distances amount to 3.2 and 3.4 Å. Since all four oxygen atoms mentioned above are strongly nucleophilic, they repel strongly at relatively small interatomic distances. Their repulsions directly influence the shape of the reaction energy profile and suppress the chemisorption minimum. A

logical conclusion would be that structural modification of the sorbent can unleash the currently inaccessible reaction.

Two other CO_2 molecules included in the same system cannot be captured chemically. They were captured electrostatically by the carboxylate moiety of PU. In both cases, the oxygen atoms of PU interact with the carbon atoms of two CO_2 molecules. Both equilibrium distances C…O equal 2.9 Å, which corresponds to the electrostatic attraction of medium strength. Table 1 summarizes thermodynamic potentials corresponding to CO_2 physisorption.

Table 1. The thermodynamic potentials of CO_2 physisorption by methylene-modified PU. The normalization of energies throughout this work is provided per one mole of CO_2.

Temperature, K	Pressure, bar	dG, kJ/mol	dH, kJ/mol	-TdS, kJ/mol	dS, J/mol/K
280	standard	23.50	-7.95	31.45	-112.3
290	standard	24.62	-7.83	32.45	-111.9
standard	standard	25.53	-7.74	33.27	-111.6
310	standard	26.85	-7.60	34.45	-111.1
320	standard	27.96	-7.49	35.44	-110.8
330	standard	29.06	-7.36	36.43	-110.4
standard	10	19.82	-7.74	27.56	-92.45
standard	50	15.83	-7.74	23.57	-79.05
standard	100	14.11	-7.74	21.85	-73.30
standard	200	12.39	-7.74	20.13	-67.52
standard	500	10.12	-7.74	17.86	-59.91

The physisorption is enthalpically favored and entropically forbidden over the entire temperature and pressure ranges. Elevated temperature decreases CO_2 sorption. In turn, elevated pressure fosters physisorption. The most favorable thermodynamics, in terms of Gibbs free energy, is seen at 298.15 K and 500 bar. When a more realistic pressure is applied, in a practical context, dG suffers insignificantly, with 12 kJ/mol under 200 bar and 14 kJ/mol under 100 bar. Assuming a porous structure of PU that can accommodate multiple captured gas molecules, even more favorable thermodynamics can be expected. Indeed, PU scavengers exhibit rather competitive CO_2 capacities in recent experiments.

Methylene and Ethylene Modifications of Polyurethane

Since chemisorption is impossible in PU, we modified the sorbent structure by separating oxygen and nitrogen atoms from one another using the methylene linkage and the ethylene linkage. In this way, we eliminate thermodynamically unfavorable O…O electrostatic repulsions. Figure 3 compares the physisorption by PU and two modified chemical structures.

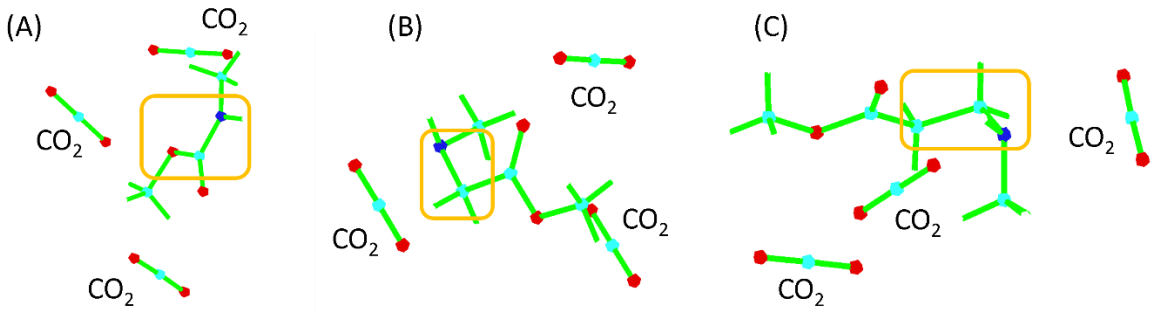

Figure 3. The optimized geometries depicting physisorption and chemisorption of CO_2 by (A) pristine PU unit; (B) modified PU by adding a methylene separator; (C) modified PU by adding an ethylene separator. The urethane linkage and its modifications are highlighted by orange rectangles.

The CO_2 molecules are coordinated by one nitrogen and two oxygen atoms. In all cases, nucleophilic centers of PU and modified PU are responsible for the observed CO_2 capture. We found that chemisorption through carboxamidation was not spontaneous. Otherwise, it would take place directly during the simulated geometry optimization following the rational-function-optimization algorithm employed. Figure 4 depicts the chemisorption of CO_2 by the methylene-modified scavenger and exemplifies the geometry of the chemisorbed CO_2 molecule at the nitrogen site.

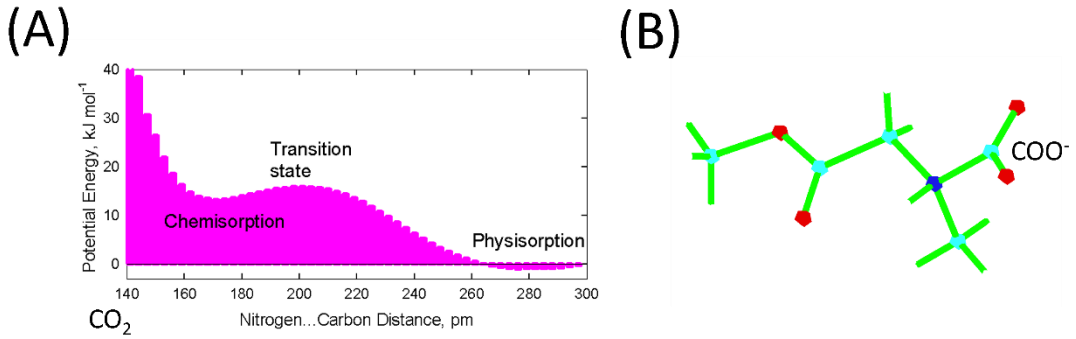

Figure 4. (A) Reaction energy profile for CO_2 chemisorption by methylene-modified structure. (B) The chemisorbed CO_2 molecule via a new PU-inspired scavenger.

The transition state is located at the reaction coordinate of 201 pm, which is C…N distance. The height of the barrier is 17 kJ/mol in terms of electronic energy. The height of an activation barrier is evaluated versus the lowest-energy state located on the right. In our case, it is a state of the CO_2 physisorption. The imaginary frequency of the saddle point amounts to i151 cm^{-1}.

The chemisorbed CO_2 state was found at the reaction coordinate of 171 pm. The energy of the simulated system relative to the physisorption energy was 14 kJ/mol. Such small involved energies suggest that CO_2 chemisorption is readily accessible even at standard conditions. In the meantime, chemisorption is enthalpically forbidden relative to physisorption. It should represent a reversible reaction that can be acceptable in the context of less expensive sorbent regeneration.

Thermochemistry of CO_2 chemisorption (Table 2) suggests that pressure increase does not boost chemisorption. Furthermore, chemisorption is entropically forbidden, although to a lesser extent than physisorption. The enthalpic gain of the carboxamidation reaction is within 1 kJ/mol versus that of CO_2 physisorption. Therefore, the chemisorption functionality was activated by a simple structural modification of the sorbent unit. A larger separating moiety can provide more efficient charge separation and enhance the chemisorption of CO_2.

Table 2. Thermochemical potentials of CO_2 chemisorption by methylene-modified PU.

Temperature, K	Pressure, bar	dG, kJ/mol	dH, kJ/mol	-TdS, kJ/mol	dS, J/mol/K
280	standard	8.55	0.43	8.12	-28.99
290	standard	8.83	0.37	8.47	-29.20
standard	standard	9.07	0.32	8.76	-29.37
310	standard	9.42	0.25	9.17	-29.57
320	standard	9.72	0.20	9.52	-29.76
330	standard	10.02	0.14	9.87	-29.92
standard	10	9.07	0.32	8.76	-29.37
standard	50	9.07	0.32	8.76	-29.37
standard	100	9.07	0.32	8.76	-29.38
standard	200	9.08	0.32	8.76	-29.38
standard	500	9.07	0.32	8.76	-29.37

Table 3 investigates the thermodynamics of CO_2 physisorption by using an ethylene-modified PU linkage. Indeed, a slight dG decrease took place. Specifically, each dG became less positive by roughly 2 kJ/mol. Although the exemplified energy gains are marginal, they signify a positive effect of spatially separating nucleophilic interaction sites from one another. Also, the effects originating from many urethane units may sum up into a substantial number for an entire PU chain.

Table 3. The thermodynamic potentials of CO_2 physisorption by ethylene-modified PU.

Temperature, K	Pressure, bar	dG, kJ/mol	dH, kJ/mol	-TdS, kJ/mol	dS, J/mol/K
280	standard	21.58	-9.84	31.41	-112.19
290	standard	22.70	-9.72	32.42	-111.79
standard	standard	23.61	-9.63	33.23	-111.47
310	standard	24.93	-9.49	34.42	-111.03
320	standard	26.04	-9.38	35.41	-110.66
330	standard	27.14	-9.26	36.40	-110.31
standard	10	17.90	-9.63	27.53	-92.32
standard	50	13.91	-9.63	23.53	-78.94
standard	100	12.19	-9.63	21.82	-73.18
standard	200	10.48	-9.63	20.10	-67.42
standard	500	8.20	-9.63	17.83	-59.79

Ethylene-modified PU is more successful in CO_2 capture (Figure 5). For instance, the chemisorption barrier decreases thrice as compared to the methylene-modified scavenger. The

state of chemisorption is more expressed versus the transition state. Two physisorption states emerge, which are linked to a more crowded molecular environment in the proximity of the nitrogen reaction site. The ethylene separator blocks strong electrostatic interactions within the PU linkage. As a result, the thermodynamic potentials favor the physisorption and chemisorption of CO_2 to a larger extent.

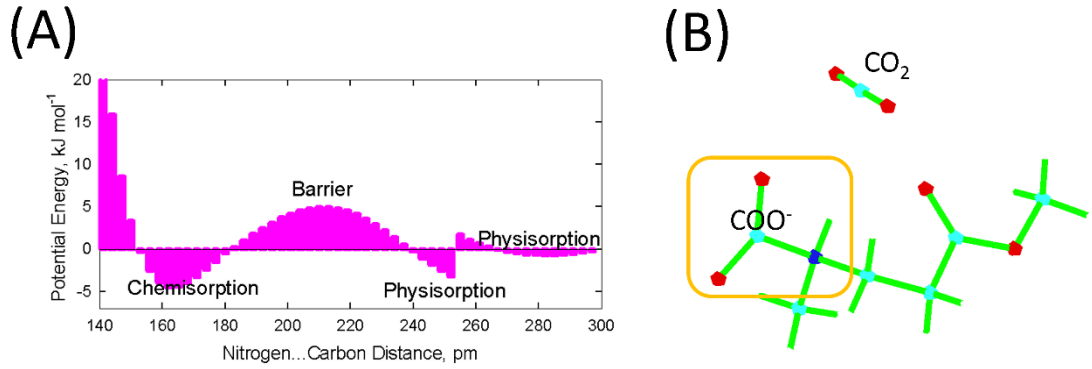

Figure 5. (A) Reaction energy profile for CO_2 chemisorption by ethylene-modified structure. (B) The chemisorbed CO_2 molecule and physisorbed CO_2 molecule via a new PU-inspired scavenger.

The imaginary frequency characterizing the transition state in the ethylene-modified PU equals 187 cm^{-1}. This is reasonably similar to the transition state in the methylene-modified PU reported in this work above. The location of the activation barrier is 210 pm. In turn, the chemisorbed CO_2 molecules can be observed at the C…N distance of 163 pm. This bond length is in excellent agreement with conventional C-N single covalent bond lengths in numerous organic compounds. Table 4 summarizes CO_2 chemisorption by the ethylene-modified novel scavenger.

Table 4. Thermochemical potentials of CO_2 chemisorption by ethylene-modified PU.

Temperature, K	Pressure, bar	dG, kJ/mol	dH, kJ/mol	-TdS, kJ/mol	dS, J/mol/K
280	standard	16.60	3.51	13.09	-46.75
290	standard	17.07	3.33	13.74	-47.39
standard	standard	17.46	3.18	14.28	-47.90
310	standard	18.03	2.97	15.06	-48.59

320	standard	18.52	2.79	15.72	-49.14
330	standard	19.01	2.62	16.39	-49.68

The CO_2 chemisorption capability, unlocked in the present work, transforms the urethane linkage into an anion. Deprotonated carbamate moiety emerges. The excess electron is localized on the oxygen atoms of carboxylate. Therefore, the stability of the system and, hence, the thermochemistry of the chemisorption reaction can be boosted in acidic media. In the reported simulations, we did not immediately include protons or counterions. Even without this sort of stabilization, the stationary points corresponding to the chemisorbed CO_2 molecules exist in both modified species.

Physisorption plays a substantial role in CO_2 capture by the modified PU scavengers, as well as by pristine PU. We hereby found three stationary points for ethylene-modified PU and CO_2 molecules (Figure 6). The stationary point, at which CO_2 coordinates the nitrogen atom of PU (C…N distance of 2.8 Å), can readily transition to the chemisorption stationary point (covalent bond length of 1.6 Å) at room conditions, according to the computed energy barriers discussed above. In turn, the states of CO_2 physisorption correspond to the electrostatic attraction of the carbon atom of CO_2 to the oxygen atoms of the carboxylate moieties.

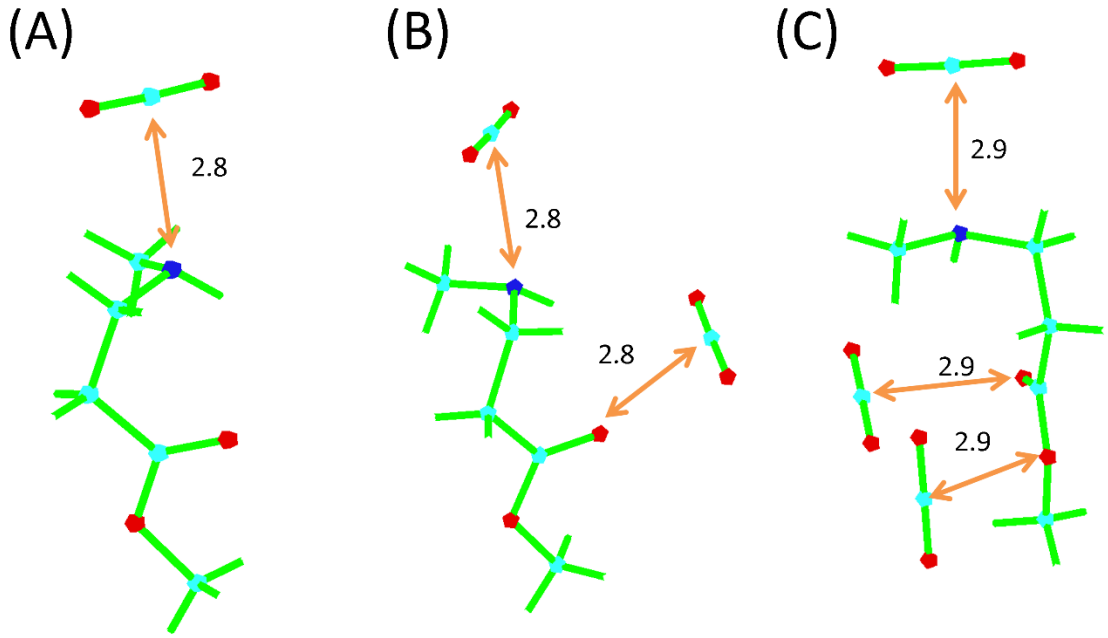

Figure 6. CO_2 physisorption geometries at ethylene-modified PU: (A) one CO_2 molecule; (B) two CO_2 molecules; (C) three CO_2 molecules. The in-plot distances are given in Ångstroms.

Atomic Nucleophilicities and Electrophilicities along the Reaction Coordinate

Figures 7-8 demonstrate how the partial atomic charges localized on the reacting centers evolve during CO_2 chemisorption. In the beginning, the carbon atom of CO_2 represents a typical electrophilic reaction center. Its partial charge equals ~0.7e. Whereas, the nitrogen atoms belonging to the methylene- and ethylene-modified PU species represent nucleophilic reaction centers.

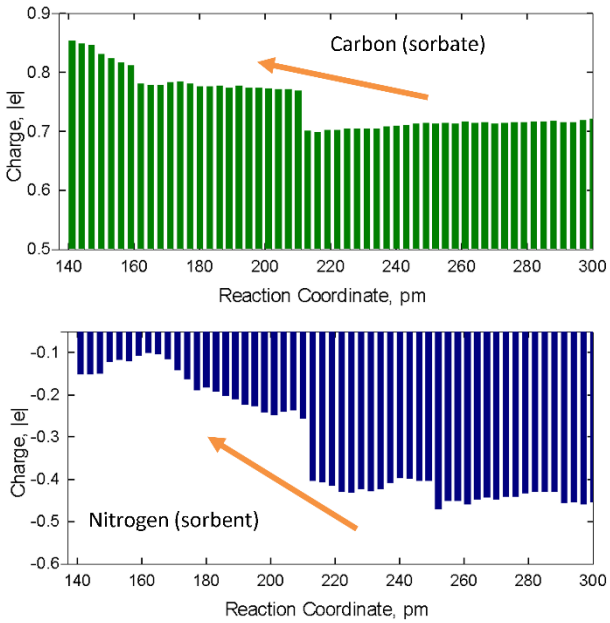

Figure 7. Partial atomic charges on the carbon and nitrogen reaction centers along the simulated CO_2 chemisorption reaction coordinate in pristine PU. The charges were computed by fitting an immediate electrostatic potential by a set of atomic coordinates.

Importantly, the case of ethylene separator turned out to be much more efficient. It increased the nucleophilicity of the nitrogen atom nearly twice compared to that in the case of the methylene separator. Compare -0.4e…-0.5e to almost -0.8e. This observation, made in terms of partial electrostatic charges, highlights that a very essential alteration in the electronic properties of PU-modified sorbent can be achieved via a tiny structural adjustment. It is also important to note that partial charges change according to different patterns along the reaction coordinates in methylene-modified and ethylene-modified sorbents.

As the reaction coordinate value approaches the state of chemisorption, the nitrogen atom of the ethylene-modified PU completely loses its initial nucleophilicity and even becomes somewhat electrophilic in the state of CO_2 chemisorption. In turn, the nitrogen atom upon methylene modification also substantially loses nucleophilicity but still retains a modest fraction of it in the state of carbamate moiety.

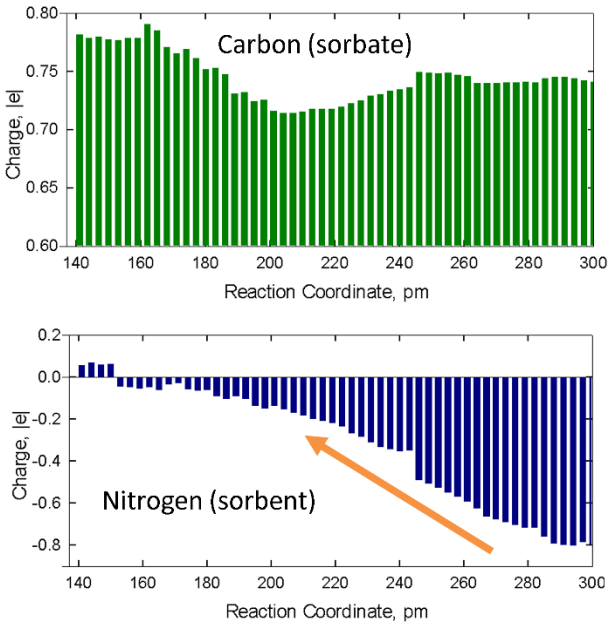

Figure 8. Partial atomic charges on the carbon and nitrogen reaction centers along the simulated CO_2 chemisorption reaction coordinate in ethylene-modified PU. The charges were computed by fitting an immediate electrostatic potential by a set of atomic coordinates.

The evolution of nucleophilicity and nucleophilicity of the directly chemically reacting atoms, nitrogen and carbon, upon their mutual approach, are in full agreement with the corresponding reaction energy profiles. These results suggest that an ethylene separator is most efficient in circumventing O…O undesirable repulsions on the way of carbamate synthesis.

Chemisorption Activation Barriers versus Temperature

The transition state represents the first-order saddle point, in which all forces are negligible. All descriptors characteristic of any stationary point apply to the transition state point. The activation energy barrier is a difference between the stational point energy and the closest minimum point energy. Tables 5-6 investigate how CO_2 chemisorption activation barriers depend on the temperature of the reaction. They also include zero-point energy corrections.

Table 5. Activation barriers of CO_2 chemisorption by methylene-modified PU. The effect of pressure is marginal in the usually experimentally used range of 1-200 bar.

Temperature, K	Pressure, bar	dG, kJ/mol	dH, kJ/mol	-TdS, kJ/mol	dS, J/mol/K
280	standard	24.68	15.33	9.35	-33.41
290	standard	25.02	15.21	9.81	-33.83
standard	standard	25.30	15.11	10.18	-34.16
310	standard	25.71	14.97	10.74	-34.63
320	standard	26.05	14.85	11.20	-35.00
330	standard	26.40	14.73	11.67	-35.36

The computed energy barriers are fairly small in all cases. It is obvious after the analysis of the thermodynamic tables that ethylene-modified PU outperforms methylene-modified PU by about 6 kJ/mol. Temperature increase insignificantly deteriorates the chemisorption reaction page through elevating barriers. In turn, the effect of pressure was found to be marginal (not shown). Mind, however, that pressure does influence CO_2 physisorption, as we discussed above.

Table 6. Activation barriers of CO_2 chemisorption by ethylene-modified PU. The effect of pressure is marginal in the usually experimentally used range of 1-200 bar.

Temperature, K	Pressure, bar	dG, kJ/mol	dH, kJ/mol	-TdS, kJ/mol	dS, J/mol/K
280	standard	18.61	10.31	8.30	-29.64
290	standard	18.90	10.21	8.70	-29.99
standard	standard	19.15	10.13	9.02	-30.27
310	standard	19.51	10.01	9.50	-30.64
320	standard	19.82	9.91	9.90	-30.95
330	standard	20.13	9.82	10.31	-31.24

Conclusions and Final Considerations

In the present work, a new CO_2 scavenger was elaborated by unlocking the chemisorption capability of PU. Specifically, thermodynamically unfavorable oxygen-oxygen repulsive interactions due to the rigidity of the sorbent's structure were identified by recording a minimum-energy reaction path and eliminated. Small separators, like methylene and ethylene groups, were inserted between the nitrogen and carbon atoms of the PU backbone. As a result, a new stationary

point emerged in the simulated system corresponding to a chemically linked CO_2 molecule to the urethane linkage.

CO_2 chemisorption follows a well-known mechanism of carboxamidation. Whereas the added performance of the sorbents brings only 5 kJ/mol of energy to the system in the case of the ethylene bridge and even weakens the stability of the simulated system in the case of the methylene bridge, a novel functionality of the scavenger contributes to the CO_2 sorption flexibility and versatility. The physisorption of CO_2 by the new sorbents is slightly exothermic, whereas the chemisorption effect is very close to zero. All reactions are entropically forbidden which is usual for gas sorption processes.

The ab initio simulations reveal that three CO_2 molecules can be fixed by one unit of each of the new scavengers. Herewith, two gas molecules are physisorbed thanks to O…C electrostatic coupling, and one gas molecule is chemisorbed thanks to the covalent N-C bond. CO_2 physisorption is corroborated by its equilibrium distances from the sorbents, which are inferior to 3 Å. The drawback of the new materials is the inability to directly synthesize them out of PU. Indeed, methylene and ethylene moieties cannot be directly inserted to separate oxygen and nitrogen from the urethane linkage. In the meantime, such separators represent thermodynamically stable structures and in no way undermine the stabilities of the exemplified scavengers as compared to PU. Synthetic efforts are hereby urged to verify the effects of the modified PU structures on scavengers' performance.

Conflict of Interest

The author hereby declares no financial interests and professional connections that might bias the interpretations of the obtained results.

Data Availability Notice

The data supporting this article have been included in the publication.

Credit Author Statement

V.V.C.: Conceptualization; Methodology Development; Validation; Formal analysis; Investigation; Resources; Data Curation; Writing - Original Draft; Writing - Review & Editing; Visualization Preparation; Supervision; Project administration.

References

1. Chaban, V. V.; Andreeva, N. A. Combating Global Warming: Moderating Carbon Dioxide Concentration in the Earth's Atmosphere through Robust Design of Novel Scavengers. LAP LAMBERT Academic Publishing, **2018**, 164 pages. isbn: 9786137327098.

2. Andreeva, N. A.; Chaban, V. V. Electronic and thermodynamic properties of the amino- and carboxamido-functionalized C-60-based fullerenes: Towards non-volatile carbon dioxide scavengers. Journal of Chemical Thermodynamics, **2018**, 116, 1-6, 10.1016/j.jct.2017.08.019.

3. Chaban, V. The thiocyanate anion is a primary driver of carbon dioxide capture by ionic liquids. Chemical Physics Letters, **2015**, 618, 89-93, 10.1016/j.cplett.2014.11.008.

4. Shen, M.; Guo, W.; Tong, L.; Wang, L.; Chu, P. K.; Kawi, S.; Ding, Y. Behavior, mechanisms, and applications of low-concentration CO2 in energy media. Chemical Society Reviews, **2025**, 10.1039/d4cs00574k.

5. Andreeva, N. A.; Chaban, V. V. Amino-functionalized ionic liquids as carbon dioxide scavengers. Ab initio thermodynamics for chemisorption. The Journal of Chemical Thermodynamics, **2016**, 103, 1-6, 10.1016/j.jct.2016.07.045.

6. Bernard, F. L.; Dalla Vecchia, F.; Rojas, M. F.; Ligabue, R.; Vieira, M. O.; Costa, E. M.; Chaban, V. V.; Einloft, S. Anticorrosion Protection by Amine–Ionic Liquid Mixtures: Experiments and Simulations. Journal of Chemical & Engineering Data, **2016**, 61 (5), 1803-1810, 10.1021/acs.jced.5b00996.

7. Wolf, M. E.; Vandezande, J. E.; Schaefer, H. F. Catalyzed reaction of isocyanates (RNCO) with water. Physical Chemistry Chemical Physics, **2021**, 23 (34), 18535-18546, 10.1039/d1cp03302f.

8. Maciel, V. G.; Bockorny, G.; Domingues, N.; Scherer, M. B.; Zortea, R. B.; Seferin, M. Comparative Life Cycle Assessment among Three Polyurethane Adhesive Technologies for the Footwear Industry. ACS Sustainable Chemistry and Engineering, **2017**, 5 (9), 8464-8472, 10.1021/acssuschemeng.7b02516.

9. Favero, D.; Marcon, V. R. R.; Barcellos, T.; Gómez, C. M.; Sanchis, M. J.; Carsí, M.; Figueroa, C. A.; Bianchi, O. Renewable polyol obtained by microwave-assisted alcoholysis of epoxidized soybean oil: Preparation, thermal properties and relaxation process. Journal of Molecular Liquids, **2019**, 285, 136-145, 10.1016/j.molliq.2019.04.078.

10. Zhang, Z.; Mei, H.; Wang, Q.; Li, R.; Wang, G.; Wei, H.; Ouyang, X. Self-healing polyurethane elastomer based on 2-ureido-4[1H]-pyrimidinone. Materials Chemistry and Physics, **2022**, 285, 126070, 10.1016/j.matchemphys.2022.126070.

11. Zhuang, G.; Wang, J.; Yang, J.; Ma, Y.; Zhang, Y.; Wang, H.; Ji, G. Polysulfide polyurethane-urea(PSPU)-based self-healing dielectric composites with poly-dopamine and KH550 chemically modified carbon nanotubes. European Polymer Journal, **2023**, 188, 111944, 10.1016/j.eurpolymj.2023.111944.

12. Olietti, A.; Pargoletti, E.; Diona, A.; Cappelletti, G. A novel optimized mold release oil-in-water emulsion for polyurethane foams production. Journal of Molecular Liquids, **2018**, 261, 199-207, 10.1016/j.molliq.2018.03.122.

13. Jamsaz, A.; Goharshadi, E. K. Flame retardant, superhydrophobic, and superoleophilic reduced graphene oxide/orthoaminophenol polyurethane sponge for efficient oil/water separation. Journal of Molecular Liquids, **2020**, 307, 112979, 10.1016/j.molliq.2020.112979.

14. Bernard, F. L.; Polesso, B. B.; Cobalchini, F. W.; Donato, A. J.; Seferin, M.; Ligabue, R.; Chaban, V. V.; do Nascimento, J. F.; Dalla Vecchia, F.; Einloft, S. CO2 capture: Tuning cation-anion interaction in urethane based poly(ionic liquids). Polymer, **2016**, 102, 199-208, 10.1016/j.polymer.2016.08.095.

15. Zhou, M.; Zhao, S.; Zhou, K.; Mei, F.; Qian, X.; Shi, C. Flexible polyurethane foams surface-modified with FeOOH for improved oil-water separation and flame retardancy. Materials Chemistry and Physics, **2022**, 276, 125408, 10.1016/j.matchemphys.2021.125408.

16. Bernard, F. L.; Dos Santos, L. M.; Cobalchina, F. W.; Schwab, M. B.; Einloft, S. Polyurethane/poly (ionic liquids) cellulosic composites and their evaluation for separation of CO2 from natural gas. Materials Research, **2019**, 22, e20180827, 10.1590/1980-5373-MR-2018-0827.

17. Bernard, F. L.; dos Santos, L. M.; Schwab, M. B.; Polesso, B. B.; do Nascimento, J. F.; Einloft, S. Polyurethane-based poly (ionic liquid)s for CO 2 removal from natural gas. Journal of Applied Polymer Science, **2019**, 136 (20), 47536, 10.1002/app.47536.

18. Singh, U. C.; Kollman, P. A. An approach to computing electrostatic charges for molecules. Journal of Computational Chemistry, **1984**, 5 (2), 129-145, 10.1002/jcc.540050204.

19. Guggenheim, H. A. Thermodynamics: An advanced treatment for chemists and physicists. 8th ed.; Elsevier: New York, **1986**, pages. isbn: 978-0444869517.

20. Peverati, R.; Truhlar, D. G. Performance of the M11 and M11-L density functionals for calculations of electronic excitation energies by adiabatic time-dependent density functional theory. Physical Chemistry Chemical Physics, **2012**, 14 (32), 11363-11370, 10.1039/C2CP41295K.

21. Weigend, F.; Ahlrichs, R. Balanced basis sets of split valence, triple zeta valence and quadruple zeta valence quality for H to Rn: Design and assessment of accuracy. Physical chemistry chemical physics : PCCP, **2005**, 7 (18), 3297-3305, 10.1039/b508541a.

22. Schmidt, M. W.; Baldridge, K. K.; Boatz, J. A.; Elbert, S. T.; Gordon, M. S.; Jensen, J. H.; Koseki, S.; Matsunaga, N.; Nguyen, K. A.; Su, S.; Windus, T. L.; Dupuis, M.; Montgomery, J. A. General atomic and molecular electronic structure system. Journal of Computational Chemistry, **1993**, 14 (11), 1347-1363, 10.1002/jcc.540141112.

23. Hanwell, M. D.; Curtis, D. E.; Lonie, D. C.; Vandermeersch, T.; Zurek, E.; Hutchison, G. R. Avogadro: an advanced semantic chemical editor, visualization, and analysis platform. Journal of Cheminformatics, **2012**, 4 (1), 17, 10.1186/1758-2946-4-17.